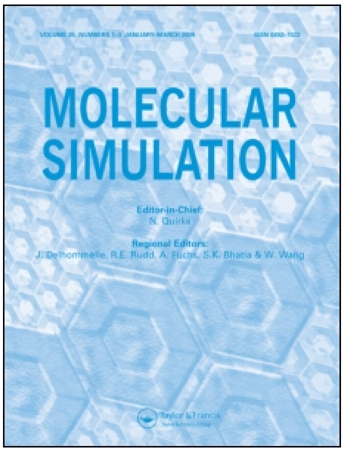

Molecular Simulation
Publication details, including instructions for authors and subscription information:
http://www.informaworld.com/smpp/title~content=t713644482

Hybrid approach for generating realistic amorphous carbon structure using metropolis and reverse Monte Carlo

George Opletal[a]; Tim Petersen[a]; Brendan O'Malley[a]; Ian Snook[a]; Dougal G. McCulloch[a]; Nigel A. Marks[b]; Irene Yarovsky[a]
[a] Department of Applied Physics, RMIT University, Melbourne, Vic., Australia [b] Department of Applied Physics, School of Physics (A28), University of Sydney, Sydney, NSW, Australia

To cite this Article Opletal, George , Petersen, Tim , O'Malley, Brendan , Snook, Ian , McCulloch, Dougal G. , Marks, Nigel A. and Yarovsky, Irene(2002) 'Hybrid approach for generating realistic amorphous carbon structure using metropolis and reverse Monte Carlo', Molecular Simulation, 28: 10, 927 — 938

To link to this Article: DOI: 10.1080/089270204000002584

URL: http://dx.doi.org/10.1080/089270204000002584

Molecular Simulation, 2002 Vol. 28 (10–11), pp. 927–938

Taylor & Francis
Taylor & Francis Group

HYBRID APPROACH FOR GENERATING REALISTIC AMORPHOUS CARBON STRUCTURE USING METROPOLIS AND REVERSE MONTE CARLO

GEORGE OPLETAL[a,*], TIM PETERSEN[a], BRENDAN O'MALLEY[a],
IAN SNOOK[a], DOUGAL G. MCCULLOCH[a], NIGEL A. MARKS[b] and
IRENE YAROVSKY[a]

[a]*Department of Applied Physics, RMIT University, P.O. Box 2476V, Melbourne, Vic. 3001, Australia;* [b]*Department of Applied Physics, School of Physics (A28), University of Sydney, Sydney, NSW 2006, Australia*

(Received May 2001, in final form November 2001)

An improved method for the modelling of carbon structures based on a hybrid reverse Monte Carlo (HRMC) method is presented. This algorithm incorporates an accurate environment dependent interaction potential (EDIP) in conjunction with the commonly used constraints derived from experimental data. In this work, we compare this new method with other modelling results for a small system of 2.9 g/cc amorphous carbon. We find that the new approach greatly improves the structural description, alleviating the common problem in standard reverse Monte Carlo method (RMC) of generating structures with a high proportion of unphysical small rings. The advantage of our method is that larger systems can now be modelled, allowing the incorporation of mesoscopic scale features.

Keywords: Reverse Monte Carlo; Carbonaceous solids; Environmental potential; Hybrid reverse Monte Carlo

INTRODUCTION

Carbon can form a vast number of natural or synthetically generated compounds including the highly anisotropic hexagonal phase graphite, tetrahedrally bonded

---

*Corresponding author.

ISSN 0892-7022 © 2002 Taylor & Francis Ltd
DOI: 10.1080/0892702021000002584

diamond, Buckminster Fullerenes and bucky tubes, naturally occurring spherical graphite [1,2] and many disordered forms. Energy calculations of toroidal forms of graphite [3] and even negatively curved graphitic sheets [4], support the physical possibility of these exotic and interesting structures.

Disordered carbon-based solids are an extremely important class of materials that are found in a wide variety of industrial applications. For example, porous carbons are used in adsorption, filtration and purification, glassy carbon is used for crucibles, carbon fibres for strengthening materials, diamond-like amorphous carbon films are employed as hard, wear resistant coatings while coals, coke and chars are of great importance as a fuel and feedstock. Accurate models of disordered carbon-based materials are essential for the further development of these materials and are crucial to our current understanding of the physical behaviour of existing materials. However, modelling of these systems has proved difficult, mainly due to the configurational bonding flexibility of carbon, the lack of crystalline order and the presence of porosity in most of these materials.

In this paper, we employ and further extend the reverse Monte Carlo (RMC) [5] algorithm to model the structure of disordered carbon materials. The RMC technique has been used extensively to produce atomic configurations based upon the fitting of experimental diffraction data. In particular, the procedure involves fitting to experimental and computationally generated radial distribution functions and/or structure factors. Although the resulting generated structural configurations fit this diffraction data within the experimental error, several authors have reported unrealistically large populations of three or four-membered rings as an artefact of the application of the standard RMC method [6,7,8]. Small ring structures represent highly strained atomic configurations with energies high enough as to forbid the production of large populations, even in a system far from equilibrium.

The unrealistic nature of the observed RMC configurations is confirmed when the results are compared to our previous Car–Parrinello *ab initio* molecular dynamics (CPMD) simulations [9] performed at the same density, which generated structures with very small numbers of three and four-membered rings. To address this issue, Walters *et al.* [6] conducted RMC simulations of 2.9 g/cc tetrahedral amorphous carbon (ta-C) with the inclusion of a “triplet” constraint to eliminate three-membered rings from their configurations. Upon imposition of the constraint, they observed the systematic reduction of three-membered rings, which were, however, replaced with an unrealistically high number of four member rings. The authors explained that these results are an intrinsic consequence of the RMC algorithm, which is biased in its production of small rings.

Another approach in the RMC modelling of carbon is to introduce a coordination constraint. This approach has been used with some success by O'Malley *et al.* [10] in the modelling of low-density graphitic carbons where this constraint forced the structure to favour three-fold coordinated atoms. Following this work, Pikunic *et al.* [11] introduced a bond angle constraint which forced the bond angle distribution to be centred about 120°, eliminating the small peak at 60° as reported by O'Malley *et al.* [10], thus implying the removal of three-membered rings from the model. However, such an arbitrary geometric constraint is not based on any experimental or theoretical evidence and does not necessarily improve the overall ring statistics.

In this work, we present a more general and physically motivated approach to modelling carbonaceous solids, which addresses the above problems. Rather than imposing arbitrary geometric constraints in the modelling algorithm, the method described here utilises a realistic empirical inter-atomic potential for carbon.

METHOD

Basic RMC Algorithm

The algorithm used in the RMC method is a variation of the Metropolis Monte Carlo method (MMC) for the calculation of ensemble averages of thermodynamic properties of a system of molecules e.g. pressure or internal energy [12]. In a Monte Carlo simulation configurations are chosen so as to produce a set of configurations with a Boltzmann distribution of energies. In RMC simulations, the difference between the experimental and calculated $S(q)$ is the quantity to be minimised, χ^2, which is given by,

$$\chi_c^2 = \sum_{i=1}^{N_{\mathrm{exp}}} \frac{(S(q_i)_{\mathrm{C}} - S(q_i)_{\mathrm{exp}})^2}{\sigma_{\mathrm{exp}}(q_i)^2} \tag{1}$$

where the subscripts c and exp refer to the static structure factor from the RMC configurations and experiment, respectively. N_{exp} is the number of experimental data points and σ_{exp} is an estimate of the experimental error.

The simulation starts with an arbitrary initial configuration of atoms. An atom is randomly selected and moved a random distance. The new $S(q)$ of the configuration of atoms is calculated as well as χ^2. If the new error, χ^2_{new}, is less than the old error, χ^2_{old}, i.e. the agreement between the experimental and configuration $S(q)$ is improved by the move, then the move is accepted and another move made. If the error is increased by the move, it is not rejected outright but accepted with a probability $\exp[-(\chi^2_{\mathrm{new}} - \chi^2_{\mathrm{old}})/2]$. The process is

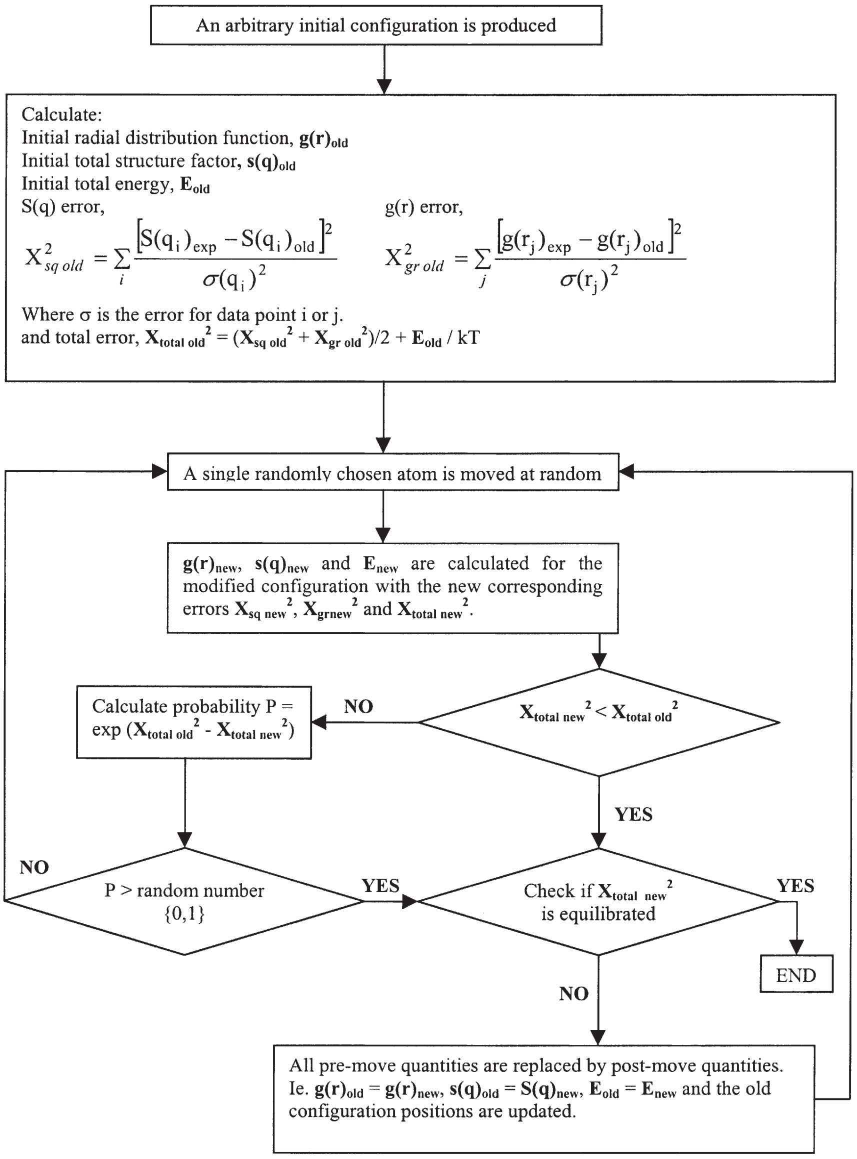

FIGURE 1 Flowchart describing the hybrid RMC method employed in this work.

then repeated until χ^2 fluctuates about an equilibrium value. This method of minimising the difference between the experimental $S(q)$ and one calculated from a three-dimensional generated structure ensures that the process neither is unlikely to get trapped into a local minima nor is overly dependent on the initial choice of starting configuration. In addition to $S(q)$ fitting, simultaneous minimisation of an error associated with the radial distribution function $g(r)$ has been shown to improve structural accuracy [13].

Hybrid Approach

In this work, an additional constraint is imposed in the form of an inter-atomic energy term, which penalises against physically unrealistic local structures, such as the highly strained and energetically unfavourable three and four member rings. The inclusion of this term into the basic RMC algorithm is schematically presented in the flow diagram (Fig. 1).

The modified RMC acceptance criterion allows for structural simulation via three methods,

- RMC energy constraint INACTIVE, $S(q)$, $g(r)$ and other constraints ACTIVE
- Metropolis Monte Carlo (MMC) energy constraint ACTIVE, $S(q)$, $g(r)$ and other constraints INACTIVE
- Hybrid Reverse Monte Carlo (HRMC) energy constraint ACTIVE, $S(q)$, g(r) and other constraints ACTIVE

In addition to $S(q)$ and $g(r)$, other constraints may include a minimum approach cut-off and a fractional coordination constraint as used in previous work [10]. However, in order to asses the pure influence of the inclusion of the potential to sole pair distribution function fitting, other constraints possible in our algorithm were not employed in this work.

Upon fitting the diffraction data, it is important to ensure that the weighting factor ($\beta = 1/kT$) for the energy in the HRMC algorithm corresponds to the experimental sample temperature. Typically, a simulated structure is "melted" and "quenched" to this temperature using only MMC, after which the $g(r)$ and $S(q)$ fitting is introduced.

Interaction Potential

The interatomic potential employed in this work is the recently developed environment dependent interaction potential (EDIP) [14] for carbon which writes the total energy as a sum of on-site energies U_i given by

$$U_i = \sum_j U_2(r_{ij}, Z_i) + \sum_{j<k} U_3(r_{ij}, r_{ik}, \theta_{jik}, Z_i) \qquad (2)$$

The two-body (U_2) and three bond (U_3) terms each in turn depend on the atomic coordination Z_i which is in general non-integral. The dominant contribution to Z_i is a spherical coordination component z_i expressed as a sum over the neighbours of i, weighted by a function of distance which is unity for small separations and decreases smoothly to zero at 2.27 Å. The full expression for the Z_i including aspherical terms is

$$Z_i = z_i + \pi_3(z_i)X_i^{dih} + \pi_3(z_i)X_i^{\mathrm{rep3}} + \pi_2(z_i)X_i^{\mathrm{rep2}} \tag{3}$$

where the X_i terms represent various geometrical constraints resulting from the interaction of sp and sp^2 π orbitals and these terms are themselves weighted via the π switching functions.

Figure 2 shows the manner in which vector products, defined within the X_i functions, smoothly enforce particular geometric constraints, where the broken lines represent positions of higher energy. The first diagram shows the dihedral term X_i^{dih}, penalising overlap from the π orbitals extending across the $m - j$ and $i - j$ atoms while the second and third diagrams shows out of plane and in plane orbital repulsion which results ideally in planar sp^2 and linear sp atoms.

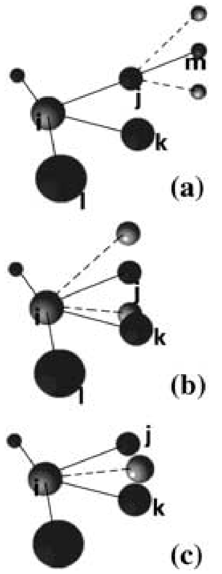

FIGURE 2 Illustration of the manner in which vector products, defined within the X_i functions, smoothly enforce particular geometric constraints, where the broken lines represent positions of higher energy for the EDIP potential [14] (see text).

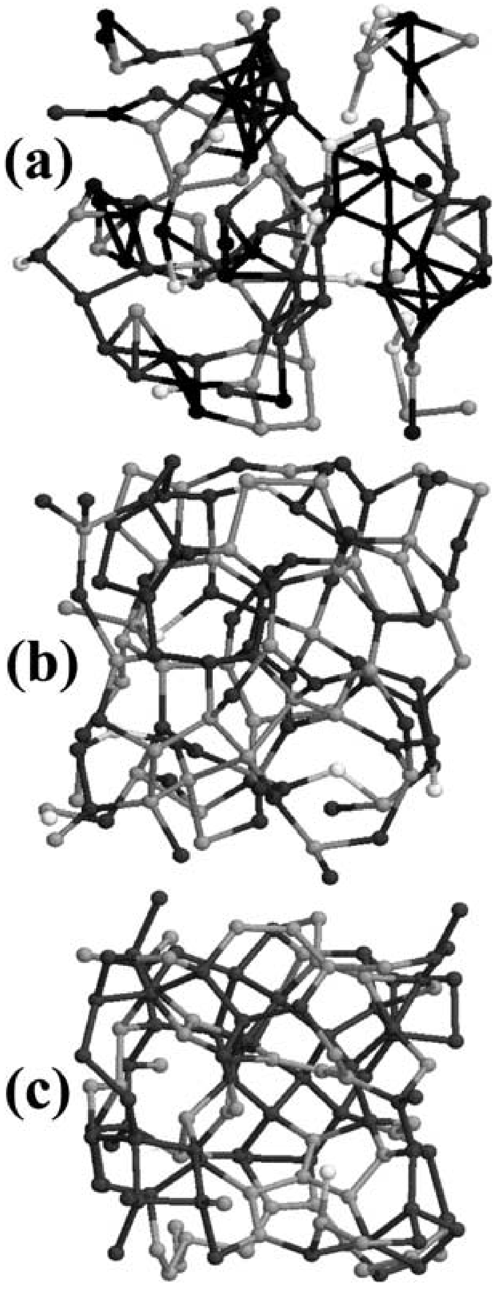

FIGURE 3 Snapshots of the final configurations generated using (a) RMC, (b) HRMC and (c) CPMD. The white atoms are two-fold coordinated, grey atoms are three-fold coordinated and dark atoms are four-fold coordinated.

RESULTS AND DISCUSSION

In order to evaluate the new algorithm, we have performed a series of simulations on a 2.9 g/cc, 125 carbon atom system for direct comparison with our CPMD results. Simulations were repeated using a variety of initial structures, including even a simple cubic lattice, resulting in statistically identical final configurations. This was done to confirm the validity of the equilibration procedure.

The same system was treated via three separate simulations approaches, as defined below:

- RMC—simulation equilibrated over 800,000 steps with the experiment error $\sigma_{\text{exp}} = 0.03$ in both the $g(r)$ and $S(q)$ fits without any constraints upon the coordination.
- MMC—simulation equilibrated at a temperature of 5000 K within 400,000 steps, after which the temperature was reduced to 300 K for a further 400,000 steps.
- HRMC—simulation equilibrated at a temperature of 5000 K within 400,000 steps, after which the temperature was reduced to 300 K and the $g(r)$ and $S(q)$ constraints ($\sigma_{\text{exp}} = 0.03$) activated for the remaining 400,000 steps. The total error reached equilibrium near 600,000 steps.

Figure 3 shows the resulting networks for the (a) RMC, (b) HRMC compared to the (c) CPMD simulation performed by McCulloch *et al.* [9]. The HRMC and CPMD results appear very similar. The RMC network exhibits unphysical bonding arrangements. Table I shows coordination numbers obtained from different runs including a comparison with CPMD results. It can be seen that the MMC and HRMC methods produced very similar results that are also in reasonable agreement with CPMD. Clearly, the RMC results deviate strongly from all other methods.

Figure 4 details the population statistics of various ring sizes defined by the shortest path criterion of Franzblau [15], obtained by simulations RMC, MMC and HRMC. Our previous results generated by the CPMD method for the same system [9] are also shown for comparison. It is apparent that the three-membered ring statistics improved significantly as a result of inclusion of the interatomic potential and the HRMC compares favourably with the CPMD results. As expected, the MMC also produced similar results. The absence of small-membered rings is a consequence of the manner in which the three-body term in the EDIP overly penalises very small angles [14]. All other ring statistics are in line with the CPMD results.

TABLE I A summary of the number of three-membered rings and coordination statistics for the three simulations performed in this work. For comparison, the results from CPMD [9] and the EDIP molecular dynamics simulations of Marks [14] are also shown. The coordination shell radius was 1.85 Å

		Coordination (%)			
Simulation method	Number of three-membered rings	2	3	4	Other
RMC	81	14	28	28	30
MC	1	2	57	41	0
HRMC	1	6	56	38	0
CPMD [9]	2	1	42	57	0
EDIP MD [14]	0	1	49	50	0

In order to further illustrate the limitations of the traditional RMC method as applied to amorphous carbon, we also performed an independent series of simulations and plotted the acceptance ratio versus the number of three-membered rings in Fig. 5. There is a clear bias for small rings as it is apparent that more configurational moves, as required to produce a good fit to the data, are possible if the proportion of small rings is increased. Thus it is evident that fitting only the diffraction data does not introduce sufficient physical restriction upon the ring size distribution and fails to produce a realistic model of high-density amorphous carbon.

Figures 6 and 7 show the structure factor $S(q)$ and the radial distribution function $g(r)$ for each of the simulations compared to the fitted diffraction data [16]. This neutron diffraction data was obtained from a sample of ta-C at a density of 3 g/cc as determined by electron energy-loss spectroscopy (EELS). However, due to inaccuracies in the measurement of the atomic density from the

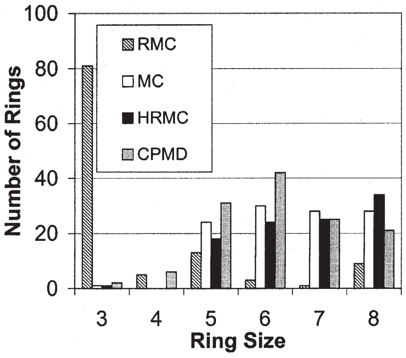

FIGURE 4 The ring statistics for the three simulations performed in this work compared to the CPMD results of McCulloch *et al.* [9].

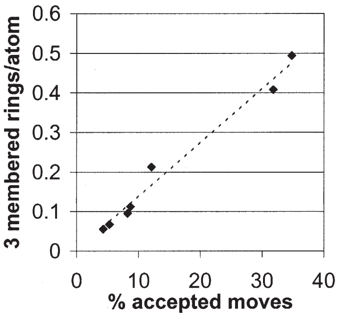

FIGURE 5 The correlation between the number of three-membered rings per atom and the RMC acceptance ratio.

position of the EELS plasmon peak, the difference between the simulated and measured densities is accounted for by the experimental error, σ_{exp}.

The configurations generated by the MMC algorithm gave the worst agreement with the experimental results. Although the ring statistics for this simulation agreed well with the CPMD result, the resulting structure is not consistent with the experimental distribution function, which demonstrates that ring statistics alone provide insufficient information to describe structural models.

Within experimental error, the results of the RMC and HRMC methods are expectedly very close to one another and in reasonable agreement with the experimental data. However, it need be stressed that fits to the experimental $S(q)$

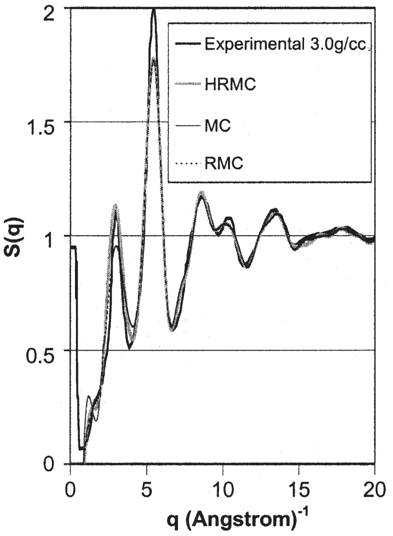

FIGURE 6 The static structure factors $S(q)$ for each of the simulated structures compared to the experimental data of Walters *et al.* [6].

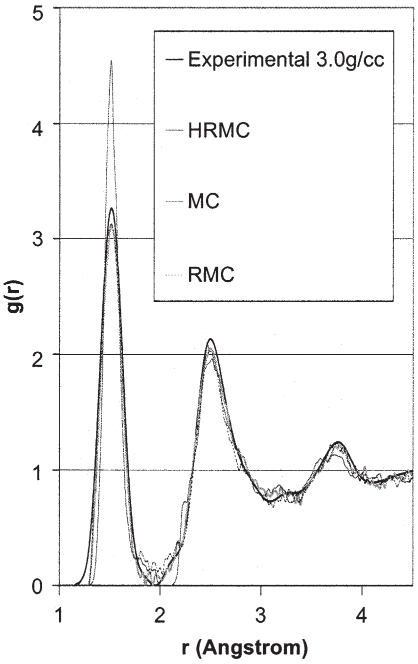

FIGURE 7 The radial distribution function $g(r)$ for each of the simulated structures compared to the experimental data of Walters *et al.* [6].

and $g(r)$ alone do not sufficiently generate realistic structural configurations for amorphous carbon systems, as indicated by the RMC ring statistics. This is to be expected for highly covalent systems such as amorphous carbons, since one-dimensional probability distribution functions, void of any angular information, cannot completely describe three-dimensional configurations.

CONCLUSION

In contrast to the imposition of arbitrary geometrical constraints upon model systems, incorporation of the EDIP potential into the RMC formalism allows physical penalisation for unrealistic local structures. Whist additional constraints to the RMC algorithm minimise the number of consistent structural configurations possible, unless experimentally or physically motivated, such constraints reduce the strength of the RMC approach. Improved ring statistics, reliable fits to experimental distribution functions and reasonable coordination numbers all indicate the superiority of the amorphous carbon structural configurations generated by the newly proposed hybrid-RMC method. Future work will include simulations of much larger systems of up to 100,000 atoms, incorporating larger scale features into our structural models.

Acknowledgements

The authors would like to acknowledge Nick Cooper for his help in code testing. One of the authors, T. Petersen, would also like to thank B.H.P Steel Pty. Ltd for their financial support.

References

[1] Jaszczak, J.A. (1997) "Unusual graphite crystals from the lime crest quarry, Sparta New Jersey", *Rocks Minerals* **1**, 330.

[2] Banhart, F. and Ajayan, P.M. (1996) "Carbon onions as nanoscopic pressure cells for diamond formation", *Nature* **382**, 433.

[3] Johnson, K., Davidson, B.N., Pederson, M.R. and Broughton, J.Q. (1994) "Energetics and structure of toroidal forms of carbon", *Phys. Rev. B* **50**, 17575.

[4] Townsend, S.J., Lenosky, T.J., Muller, D.A., Nichols, C.S. and Elser, V. (1992) "Negatively curved graphitic sheet model of amorphous carbon", *Phys. Rev. Lett.* **69**, 921.

[5] McGreevy, R.L. and Pusztai, L. (1988), *Mol. Simul.* **1**, 359.

[6] Walters, J.K., Gilkes, K.W.R., Wicks, J.D. and Newport, R.J. (1988) "Progress in modeling the chemical bonding in tetrahedral amorphous carbon", *Phys. Rev. B* **58**, 8267.

[7] Gereben, O. and Pusztai, L. (1994) "Structure of amorphous semiconductors: reverse Monte Carlo studies on *a*-C, *a*-Si, and *a*-Ge", *Phys. Rev. B* **50**, 14136.

[8] Rosato, V., Lascovich, J.C., Santoni, A. and Colombo, L. (1998) "On the use of the reverse Monte Carlo technique to generate amorphous carbon structures", *Int. J. Modern Phys., C* **9**, 917.

[9] McCulloch, D.G., McKenzie, D.R. and Goringe, C.M. (2000) "*Ab initio* simulations of the structure of amorphous carbon", *Phys. Rev. B* **61**, 2349.

[10] O'Malley, B., Snook, I. and McCulloch, D.G. (1998) "Reverse Monte Carlo analysis of the structure of glassy carbon using electron-microscopy data", *Phys. Rev B* **57**, 14148.

[11] Pikunic, J., Pellenq, R.J.M., Thomson, K.T., Rouzaud, J.N., Levitz, P. and Gubbins, K.E. (2001) "Improved molecular models for porous carbons", *Stud. Surface Sci. Catal.* **132**, 647.

[12] Tildesley, D.J. and Allen, M.P. (1987) *Computer Simulation of Liquids* (Oxford Science, City).

[13] Toth, G. and Baranyai, A. (1997) "Conceptual and technical improvement of the reverse Monte Carlo algorithm", *J. Chem. Phys.* **107**, 7402.

[14] Marks, N. (2001) "Generalizing the environment-dependent interaction potential for carbon", *Phys. Rev. B* **63**, 35401.

[15] Franzblau, D.S. (1991) "Computation of ring statistics for network models of solids", *Phys Rev. B* **44**, 4925.

[16] Gilkes, K.W.R., Gaskell, P.H. and Robertson, J. (1995) "Comparison of neutron-scattering data for tetrahedral amorphous carbon with structural models", *Phys. Rev. B* **12**, 303.